http://www.kidney-international.org

© 2011 International Society of Nephrology

Proteomic identification of vanin-1 as a marker of kidney damage in a rat model of type 1 diabetic nephropathy

Tim Fugmann[1], Beatrice Borgia[1], Csaba Révész[2], Mária Godó[2], Carol Forsblom[3,4], Peter Hamar[2], Harry Holthöfer[5], Dario Neri[1] and Christoph Roesli[1]

[1]*Department of Chemistry and Applied Biosciences, Institute of Pharmaceutical Sciences, ETH Zurich, Zurich, Switzerland;* [2]*Department of Medicine, Institute of Pathophysiology, Semmelweis University, Budapest, Hungary;* [3]*Folkhälsan Research Center, Biomedicum Helsinki, Folkhälsan Institute of Genetics, Helsinki, Finland;* [4]*Division of Nephrology, Department of Medicine, Helsinki University Hospital, Helsinki, Finland and* [5]*Department of Pathology, Haartman Institute, University of Helsinki, Helsinki, Finland*

At present, the urinary albumin excretion rate is the best noninvasive predictor for diabetic nephropathy (DN) but major limitations are associated with this marker. Here, we used *in vivo* perfusion technology to establish disease progression markers in an animal model of DN. Rats were perfused with a reactive ester derivative of biotin at various times after streptozotocin treatment. Following homogenization of kidney tissue and affinity purification of biotinylated proteins, a label-free mass spectrometry-based proteomic analysis of tryptic digests identified and relatively quantified 396 proteins. Of these proteins, 24 and 11 were found to be more than 10-fold up- or downregulated, respectively, compared with the same procedure in vehicle-treated rats. Changes in the expression of selected differentially regulated proteins were validated by immunofluorescence detection in kidney tissue from control and diabetic rats. Immunoblot analysis of pooled human urine found that concentrations of vanin-1, an ectoenzyme pantetheinase, distinguished diabetic patients with macroalbuminuria from those with normal albuminuria. Uromodulin was elevated in the urine pools of the diabetic patients, regardless of the degree of albuminuria, compared with healthy controls. Thus, *in vivo* biotinylation facilitates the detection of disease-specific changes in the abundance of potential biomarker proteins for disease monitoring and/or pharmacodelivery applications.

Kidney International (2011) **80,** 272–281; doi:10.1038/ki.2011.116; published online 4 May 2011

KEYWORDS: diabetic nephropathy; diagnosis; podocyte; vascular access

Correspondence: *Christoph Roesli, Department of Chemistry and Applied Biosciences, Institute of Pharmaceutical Sciences, ETH Zurich, Wolfgang-Pauli-Strasse 10, 8093 Zurich, Switzerland.*
E-mail: christoph.roesli@pharma.ethz.ch

Received 25 March 2010; revised 20 February 2011; accepted 1 March 2011; published online 4 May 2011

Diabetes mellitus is one of the most common chronic diseases affecting 285 million patients worldwide. Classically, diabetes has been divided in two main subtypes type 1 diabetes (T1D) and type 2 diabetes (T2D), as well as secondary diabetes and some monogenic forms of diabetes.

Although T1D only accounts for 5–10% of patients, its incidence continues to increase worldwide.[1] The susceptibility for the disease is largely inherited, residing predominantly in two genotypes of the human leukocyte antigen, but it is largely unknown which factors trigger the onset of clinical symptoms.[2] After disease onset, an autoimmune reaction results in the destruction of pancreatic β-cells and in an absolute insulin deficiency.

In the etiopathology of T1D as well as T2D, several complications are likely to occur. The chronic elevation of blood glucose levels together with the lack of insulin and other metabolic consequences leads to damage of blood vessels, hence called diabetic micro- and macroangiopathy. Diabetic angiopathy of the capillaries in the kidney glomeruli is most likely involved in the general diabetic nephropathy (DN), a progressive kidney disease that is characterized by a set of structural and functional kidney abnormalities.[3] Structural abnormalities include kidney hypertrophy in the early stage of the disease, continuous overproduction of extracellular matrix leading to increased glomerular basement membrane thickness, nodular and diffuse glomerulosclerosis, tubular atrophy, and interstitial fibrosis.[4] In an early stage, the functional kidney abnormalities include hyperperfusion and intraglomerular hypertension.[5] Subsequently, increasing proteinuria, abnormalities of intraglomerular pressure regulation, systemic hypertension, and continuous decrease of glomerular filtration rate characterize DN.[6] Currently, the earliest clinical evidence of DN is microalbuminuria, which is defined as urinary albumin excretion between 30 and 300 mg/day. Without specific interventions, ~40% of subjects with T1D progress to the stage of overt nephropathy (or clinical albuminuria; defined as urinary albumin excretion >300 mg/day) over a period of 10–15

years.[7] Once overt nephropathy occurs, the glomerular filtration rate gradually falls over a period of several years if no specific treatment is started. Finally, an estimated 30–40% of type 1 diabetic patients with DN will develop end-stage renal disease within 10 years. These patients then depend on renal replacement therapy, such as peritoneal dialysis, hemodialysis, and renal transplantation.[8]

At present, the urinary albumin excretion rate (UAER) is the best noninvasive predictor for DN but major limitations are associated with this marker. Although microalbuminuria indicates declining kidney function, it is at the same time an independent risk factor for cardiovascular disease.[9] Furthermore, the presence of microalbuminuria by itself is no adequate indicator for disease progression because of the observation that 64% of 170 T1D patients reverted to normoalbuminuria without treatment within a 5-year period.[10] The same study concluded that only glomerular basement membrane thickening and increased glomerular filtration rate are predictors for disease progression. Finally, the occurrence of microalbuminuria in T1D can be associated with DN lesions comparable to the ones in overt albuminuria.[11]

To better understand the various pathophysiological features of DN and to identify potential biomarkers able to detect DN disease progression or response to therapy, a number of proteomics investigations have been carried out in the last years. The availability of rodent models of T1D and its complications, such as rats with streptozotocin (STZ)-induced DN[12] and OVE26 transgenic mice,[13] facilitate these investigations. Sharma *et al.*[14] have analyzed the urinary proteome of patients with DN and healthy controls, resulting in the identification of alpha-1 antitrypsin being 19-fold upregulated in the diabetic group. In another study, the C-reactive protein has been identified as possible serum biomarker when comparing STZ-induced diabetic rats with healthy controls.[15] The comparison of whole-kidney lysates derived from OVE26 transgenic mice with the ones of background FVB non-diabetic mice allowed the identification of tubulointerstitial elastin depositions in DN and indicated the potential value of proteomics analyses in defining features of the pathophysiological processes in diabetes.[16] Furthermore, techniques for the proteomics-based identification of differentially expressed proteins in glomeruli from mouse kidneys and human biopsies were developed, either embolizing magnetic beads into the glomerular capillaries, followed by magnetic separation of bead-filled glomeruli or by laser capture microdissection, respectively.[17] Finally, the analysis of cultured podocytes grown under different glucose concentrations contributed to the identification of novel targets involved in DN.[18]

To establish new vascular markers of pathology, our group has previously used chemical proteomic techniques, based either on the *in vivo* perfusion of tumor-bearing animals[19–22] or on the *ex vivo* perfusion of surgically resected human organs with cancer,[23,24] followed by the subsequent capture of biotinylated proteins on streptavidin resin. These studies revealed that the *in vivo* perfusion procedure facilitates the study of the vascular proteome in cancer, allowing the identification of markers of angiogenesis, which can be drugged with monoclonal antibodies.[25]

In this study, we used the *in vivo* perfusion technology to establish disease progression markers of DN in an animal model of T1D. For this, we performed a comparative proteomic analysis of the accessible proteins of kidneys in the STZ model of non-insulin-treated rats by *in vivo* protein biotinylation[20,26] and mass spectrometry-based label-free protein identification and quantification.[27,28] The accessible kidney proteomes of citrate-treated rats as well as rats terminally perfused either 4, 8, or 12 weeks after STZ injection were compared using the in-house-developed software suite DeepQuanTR.[29] The proteomic analysis resulted in the identification and relative quantification of 396 proteins, whereof 24 and 11 have been found more than 10-fold up- or downregulated, respectively. Selected differentially regulated proteins were validated by immunofluorescence detection in rat kidney tissue. Interestingly, our results show typical leakage pattern of the respective proteins into the urine of patients with T1D and different levels of DN.

RESULTS

STZ-induced rat model of DN

Following STZ injection, animals developed severe diabetes with very high postprandial blood glucose values compared with citrate-treated control animals. At 12 weeks after citrate injection, blood glucose was normal as assessed by the oral glucose tolerance test. In contrast, STZ-treated rats showed a slightly elevated glucose level after fasting and developed very high serum glucose levels following oral glucose tolerance test. The hyperglycemia was lowered only very slowly, and was still high at 2 h after glucose gavage (Supplementary Table S1 online).

Furthermore, STZ-induced diabetes resulted in severe renal damage. Urinary albumin excretion rarely exceeded 250 mg/day in citrate-treated control rats, whereas animals treated with STZ developed progressive albuminuria, reaching a UAER of 1500 mg/day (Supplementary Table S1 online). Albuminuria was accompanied by reduced renal excretory function at 12 weeks after STZ treatment. Blood urea and creatinine values were about four times higher in STZ rats compared with normal values measured in citrate-injected controls.

In vivo perfusion of rats and chemical proteomic analysis

Twenty-one-week-old rats at 4, 8, and 12 weeks after STZ treatment as well as age-matched citrate-injected control rats were subjected to a terminal perfusion procedure with a 0.5 mg/ml solution of the reactive biotin ester Sulfo-NHS-LC-biotin (Pierce, Rockford, IL), followed by a quenching step with a 50 mmol/l Tris-HCl solution. Immediately after perfusion, the renal capsules were removed, the kidneys cut in half, and the two halves separately frozen in liquid nitrogen. After the first thawing, a cross-section was cut out of the middle of each kidney half and embedded in OCT

medium for histochemical analyses, whereas the rest of the kidney was homogenized. The resulting protein extract was loaded in the presence of 2% SDS onto a streptavidin-affinity resin to purify biotinylated proteins. The following on-resin tryptic protein digestion yielded proteolytic peptides suitable for the mass spectrometry-based comparative proteomic analysis (Figure 1a). Successful biotinylation of accessible structures in the kidney was assessed by histochemical staining of biotin using the streptavidin–biotinylated alkaline phosphatase complex and fast red as phosphatase substrate (Figure 1b).

Tryptic peptides derived from the on-resin digestion of purified biotinylated proteins of individual kidneys were separated by reversed-phase nanocapillary high-performance liquid chromatography. The resulting fractions were mixed with constant amounts of four internal standard peptides and matrix, robotically spotted on MALDI-target plates (Foster City, CA) and analyzed by MALDI-TOF (Foster City, CA) and MALDI-TOF/TOF MS (Foster City, CA) for quantification and identification purposes, respectively. The DeepQuanTR analysis allowed the relative quantification of a total of 396 proteins identified with at least two proteotypic peptides (Figure 2 and Supplementary Table S2 online). The number of identified proteins is similar to experiments performed for the analysis of tumors and normal organs in mice.[20,21]

The accessible kidney proteome of STZ-treated and citrate-injected control rats

The chemical proteomic analysis revealed a number of proteins with known expression on vascular endothelial cells, in the apical and the lateral membrane area of podocytes, in the glomerular basement membrane, and in the proximal tubule (Table 1), defining therefore the kidney substructures

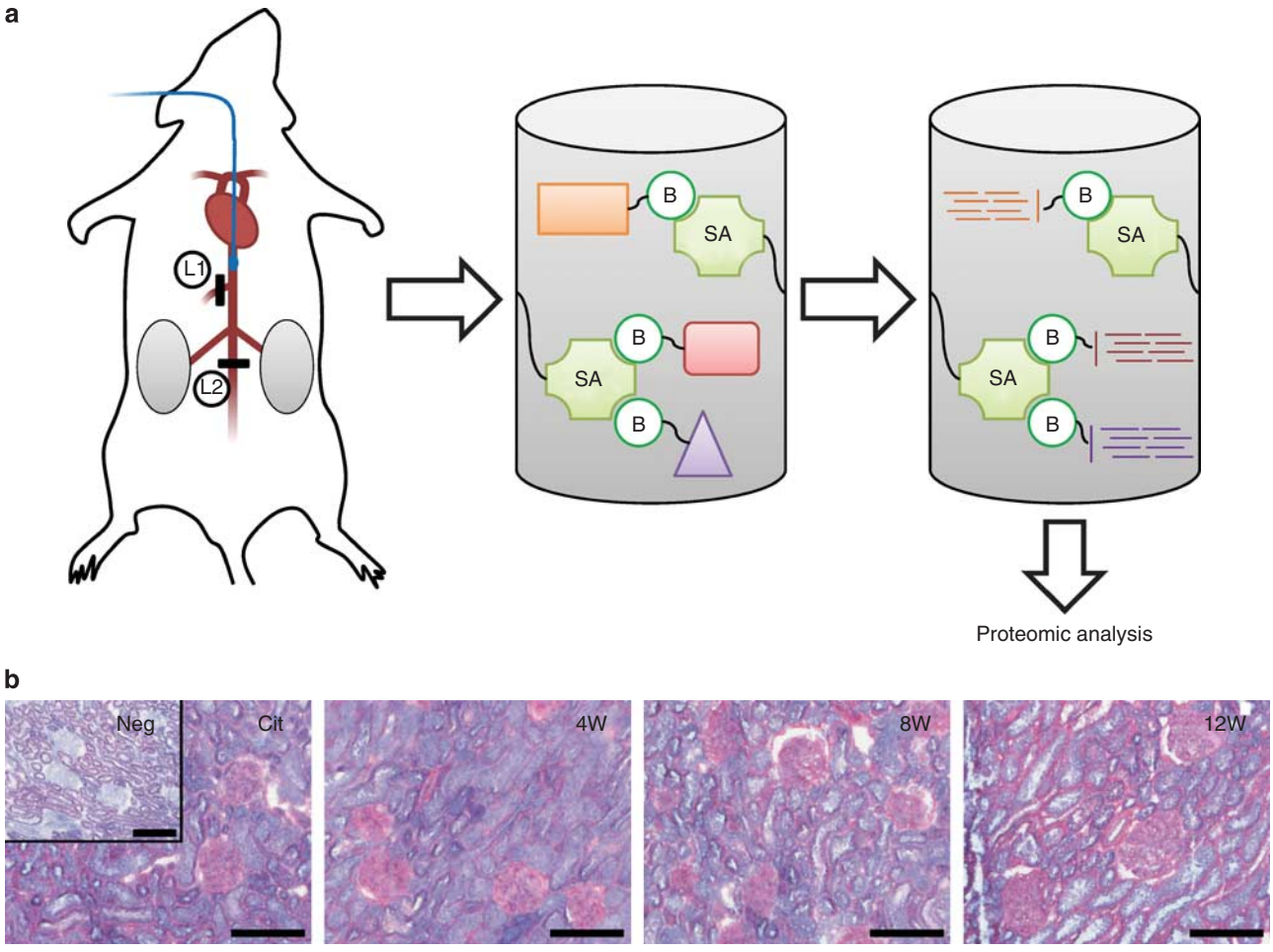

Figure 1 | Schematic depiction of the chemical proteomic workflow and validation of the *in vivo* biotinylation efficacy. (**a**) The abdomen of anesthetized rats was cut open and two ligations (L1 on the hepatic artery, L2 on the abdominal artery, and vein below the branching points of the kidney arteries) were placed. Using a buttoned cannula, the kidneys were perfused through the aorta abdominalis using a solution containing a reactive ester derivative of biotin. Following removal of the kidneys, tissue homogenization and protein extraction, biotin-tagged proteins were enriched on a streptavidin-affinity resin. A tryptic on-resin digestion resulted in proteolytic peptides submitted to the comparative proteomic analysis. B, biotin; SA, streptavidin. (**b**) The *in vivo* biotinylation efficacy was validated by a histochemical staining of biotin using the streptavidin–biotinylated alkaline phosphatase complex and fast RED. Scale bars: 200 μm. Cit, citrate-treated control; Neg, phosphate-buffered saline-perfused control rat; 4W, 8W, and 12W, 4, 8, and 12 weeks after streptozotocin treatment.

Protein name	SwissProt acc. nr.	Gene name	Peptide count	Protein quant values			
				Cit	4W	8W	12W
Vanin-1	Q4KLZ0	*Vnn1*	3	–3.56	1.82	1.64	0.09
Kininogen 1	Q5PQU1	*Kng1*	4	–3.01	0.87	0.78	1.36
Haptoglobin	P06866	*Hp*	4	–2.99	–1.50	2.68	1.82
Glutathione peroxidase 1	P04041	*Gpx1*	2	–2.36	1.81	0.44	0.11
Enpp6 protein	B0BND0	*Enpp6*	4	–2.21	–0.03	0.58	1.66
Eng protein	Q3KR75	*Eng*	5	–0.89	–0.23	0.58	0.54
Alpha-1-acid glycoprotein	P02764	*Orm1*	3	–0.89	–0.20	–0.03	1.12
Podocalyxin	Q9WTQ2	*Podxl*	2	–0.77	1.86	–0.27	–0.81
Intercellular adhesion molecule 2	Q6AXM6	*Icam2*	3	–0.76	–0.17	0.57	0.36
Decorin	Q01129	*Dcn*	8	–0.01	0.20	0.28	–0.47
CD151 antigen	Q9QZA6	*Cd151*	2	0.40	0.58	–0.31	–0.67
Alpha-actinin-4	Q9QXQ0	*Actn4*	3	0.42	–0.11	–0.19	–0.12
Kin of IRRE-like protein 1	Q6X936	*Kirrel*	6	0.43	–0.08	–0.32	–0.03
Protein tyrosine phosphatase D30	Q62797	*Ptpro*	2	0.56	0.02	–0.52	–0.07
4F2 cell-surface antigen heavy chain	Q794F9	*Slc3a2*	8	0.69	–0.46	–0.41	0.18
Neprilysin	P07861	*Mme*	3	0.74	–1.08	0.35	–0.02
Nephrin	Q9R044	*Nphs1*	5	1.28	–0.49	–0.60	–0.19
Alpha-3 type IV collagen	Q63122	*Col4a3*	2	1.39	–0.42	–0.42	–0.55
Solute carrier family 22 member 2	Q9R0W2	*Slc22a2*	4	2.63	–0.42	–1.67	–0.54
Uromodulin	P27590	*Umod*	5	3.13	–1.53	–1.29	–0.31

Figure 2 | List of selected proteins identified and quantified in this proteomic study. Besides differentially regulated proteins, a number of proteins with known contribution to glomerulus diseases (for example, nephrin, podocalyxin, and CD151 antigen) were identified. Antigens selected for further investigation are marked in bold. Protein abundances are displayed with a color code and the underlying protein quant value (the protein quant value corresponds to the natural logarithm of the fold expression change). Proteins upregulated in comparison with the average protein expression are displayed in green and downregulated proteins in red. Number of samples per group: 7. Cit, citrate-treated control; 4W, 8W, and 12W, 4, 8, and 12 weeks after streptozotocin treatment.

Table 1 | Localization of selected proteins identified in the comparative proteomic analysis of citrate-treated and STZ-induced diabetic rats

Protein name	Gene name	SwissProt acc. nr.	Location	Reference
Platelet endothelial cell adhesion molecule	*Pecam1*	Q3SWT0	EM	Woodfin and co-workers[50]
Neuropilin-1	*Nrp1*	Q9QWJ9	EM	Pellet-Many *et al.*[51]
Endothelial cell-selective adhesion molecule	*Esam*	Q6AYD4	EM	Wong *et al.*[52]
Podocalyxin	*Podxl*	Q9WTQ2	AMP	Aaltonen Holthofer[53]
Ezrin	*Ezr*	P31977	AMP	Aaltonen Holthofer[53]
Protein tyrosine phosphatase D30	*Ptpro*	Q62797	AMP	Aaltonen Holthofer[53]
Low-density lipoprotein receptor-related protein 2 (megalin)	*Lrp2*	P98158	AMP	Aaltonen Holthofer[53]
Nephrin	*Nphs1*	Q9R044	LMP	Aaltonen Holthofer[53]
Kin of IRRE-like protein 1	*Kirrel (Neph1)*	Q6X936	LMP	Aaltonen Holthofer[53]
CD151 antigen	*Cd151*	Q9QZA6	GBM	Karamatic Crew *et al.*[54]
Agrin	*Agrn*	P25304	GBM	Li *et al.*[55]
Neutral and basic amino-acid transport protein rBAT	*Slc3a1*	Q64319	PT	Raciti *et al.*[56]
Electrogenic sodium bicarbonate cotransporter 1	*Slc4a4*	Q9JI66	PT	Raciti *et al.*[56]
Sodium/glucose cotransporter 2	*Slc5a2*	P53792	PT	Raciti *et al.*[56]
Sodium-dependent neutral amino-acid transporter B(0)AT1	*Slc6a19*	Q2A865	PT	Raciti *et al.*[56]
Solute carrier family 13 member 3	*Slc13a3*	Q9Z0Z5	PT	Raciti *et al.*[56]
Solute carrier family 22 member 2	*Slc22a2*	Q9R0W2	PT	Raciti *et al.*[56]
Solute carrier family 22 member 5	*Slc22a5*	O70594	PT	Raciti *et al.*[56]
Solute carrier family 22 member 6	*Slc22a6*	O35956	PT	Raciti *et al.*[56]

Abbreviations: AMP, apical membrane area of the podocyte; EM, endothelial membrane; GBM, glomerular basement membrane; LMP, lateral membrane area of the podocyte; PT, proximal tubule; STZ, streptozotocin.

readily accessible for the charged biotinylation reagent used in the perfusion experiments. During perfusion with the reactive ester derivative of biotin and subsequently the quenching solution soluble proteins are removed from the kidneys. Out of the 396 identified and quantified proteins, 24 and 11 proteins were found more than tenfold upregulated and downregulated in the diseased kidneys compared with the citrate-treated kidneys, respectively (Supplementary Figure S1 online). Some of

these have previously been described to be involved and/or regulated in DN (Supplementary Table S3 online).

Validation of accessible targets in DN

The selection of proteins used for the validation of the DeepQuanTR results was based both on the protein regulation determined by this proteomic investigation and on the availability of antibodies recognizing the rat protein. Four differentially regulated proteins (Figure 2, bold) were selected for validation by immunofluorescence: (1) vanin-1 (*Vnn1*, upregulated in diseased), (2) Ennp6 protein (*Enpp6*, upregulated in diseased), (3) alpha-1-acid glycoprotein (*Orm1*, slightly upregulated in diseased), and (4) uromodulin (*Umod*, downregulated in diseased). The immunofluorescence analysis of rat kidney tissue derived from citrate-injected control rats and the STZ-injected diabetic rats (4, 8, and 12 weeks after STZ injection) confirmed the mass spectrometry-based findings (Figure 3). Unfortunately, vanin-1-specific antibodies that cross-react with the rat protein are not commercially available. Antibodies against *Enpp6* and

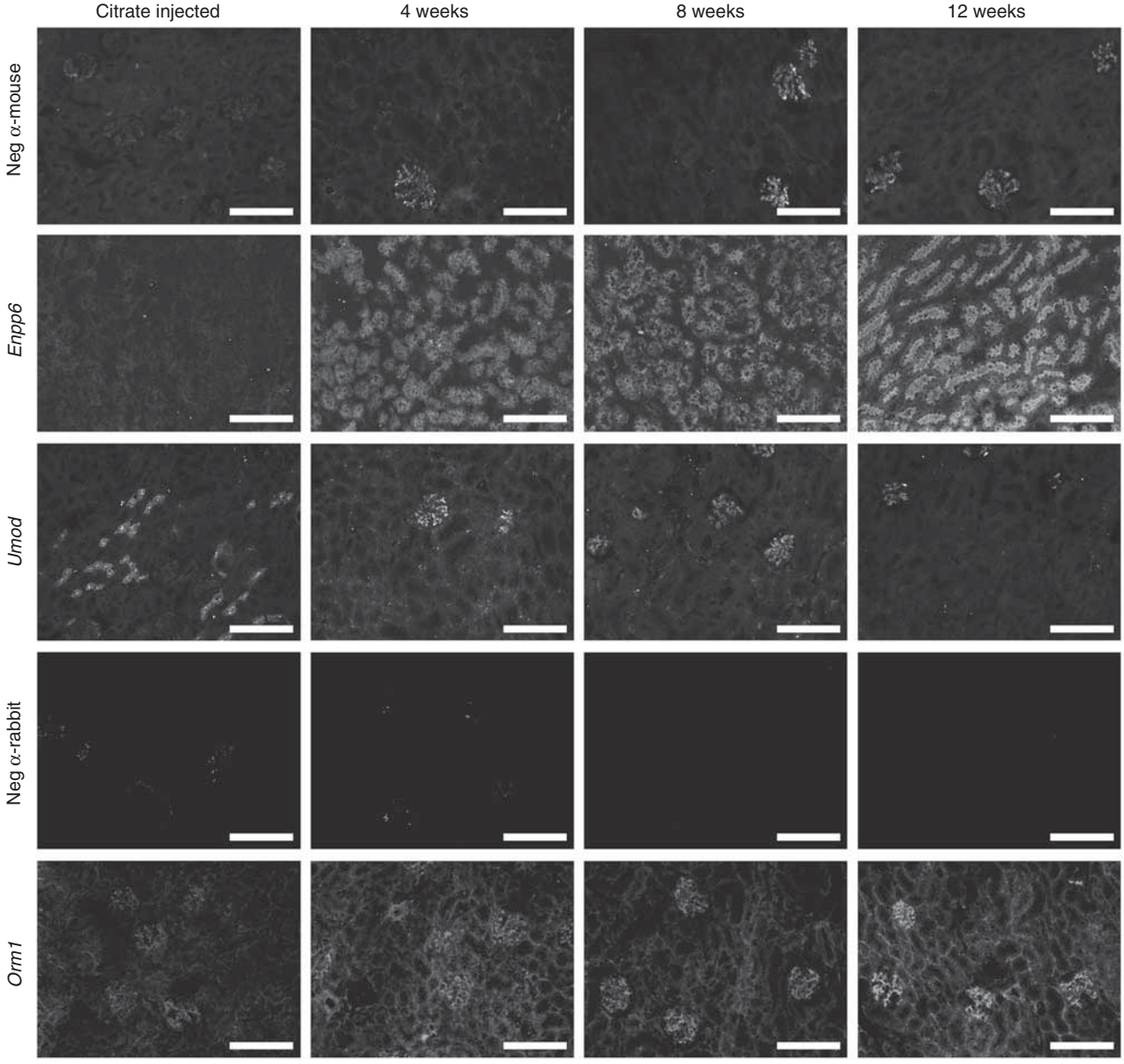

Figure 3 | Validation of DeepQuanTR results. Immunostainings of kidney sections derived from citrate-injected control rats and streptozotocin-injected diabetic rats killed at 4, 8, and 12 weeks after the end of the pharmacological treatment using antibodies against *Enpp6*, *Orm1*, and *Umod* are presented. Additionally, negative controls omitting the primary antibody are shown (using only the secondary anti-mouse antibody as negative control for *Enpp6* and *Umod*, and only the secondary anti-rabbit antibody for *Orm1*). Antibodies against *Enpp6* and *Umod* stained tubular structures, whereas *Orm1* was found in glomeruli. The differential expression of the three analyzed proteins shown by immunostaining confirmed the results obtained by the proteomic analysis. Scale bars: 200 μm. Neg, negative.

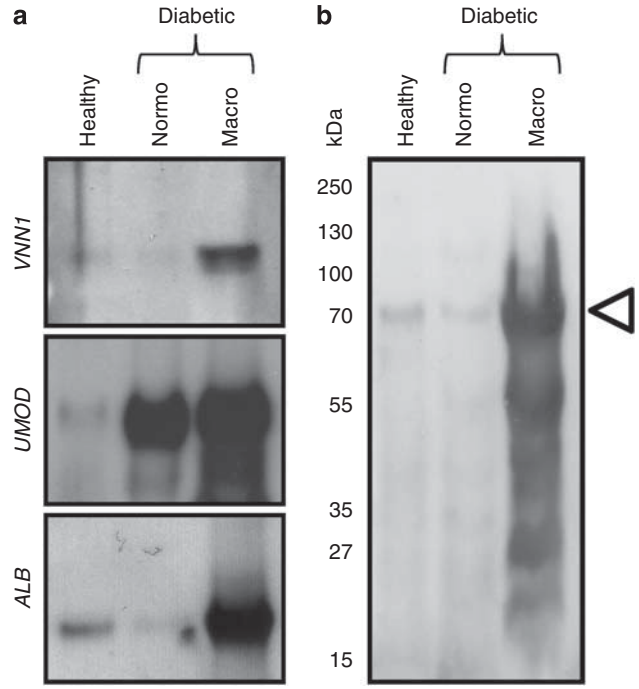

Figure 4 | Validation of selected proteins in human urine. (**a**) Western blot analyses using urine derived from healthy individuals and from diabetic patients with normal urinary albumin excretion (normo) and with macroalbuminuria (macro) were performed using antibodies against *VNN1*, *UMOD,* and *ALB*. (**b**) A Ponceau S-stained western blot of creatinine-normalized urines is shown. The albumin band is indicated with an arrowhead.

Umod stained tubular structures, whereas the anti-*Orm1* antibody stained the glomeruli.

Analysis of protein expression in human urine

To investigate whether the differential protein expression of the four selected regulated proteins could be translated to the human pathology, urine sample pools derived from healthy individuals and from T1D diabetes patients without (<30 mg/day) and with highly (>300 mg/day) elevated UAER were analyzed. To standardize the spot urine samples, all urine pools were normalized to the creatinine concentration before analysis, analogous to standard clinical procedures. Western blots of the three urine pools confirmed the upregulation of *Vnn1* and *Umod* in the macroalbuminuria samples and in the diabetic samples, respectively (Figure 4). Compared with albumin, which can be identified both in urine of healthy individuals and diabetic patients (Figure 4), uromodulin was found to be strongly upregulated in diabetic samples and vanin-1 in samples of diabetic patients with macroalbuminuria.

Analysis of protein expression in individual human urine

The urine of 6 healthy individuals and 10 diabetic patients was collected for an analysis of interindividual variability of *VNN1* and *UMOD* excretion (Figure 5a). *UMOD* levels in all diabetic patients were found to be elevated, similar to what was observed in pooled urine samples. The increase was most pronounced in diabetic patients with elevated UAER (Figure 5b). In contrast, the vanin-1 concentration in the urine samples of individual patients was found to be highly variable (Figure 5c). Patients with elevated UAER did not show a significant increase of vanin-1 concentration in the urine.

Comparison with published microarray data

To get further insight into the mechanism of protein regulation, we compared our proteomics findings with publicly available microarray data (see Supplementary Materials online).[30,31] Owing to the different nature of the samples (renal tubular cells for microarray experiments versus the cell surface proteome of endothelial cells, podocytes, and tubular cells, as well as extracellular matrix in the proximity of these cells for our proteomic study), there was no global correlation between the proteomics and the microarray data (Supplementary Figure S2 online). Noteworthy, neither *VNN1* nor *UMOD* was found to be significantly regulated in these studies. Furthermore, microarrays used in both studies lacked in probes against *ENPP6*. Although Rudnicki *et al.*[30] analyzed patient samples from proteinuric nephropathies, but not from DN, we estimate that the lack of correlation emphasizes the unique nature of the proteomics analysis presented here.

DISCUSSION

The proteomic analysis described in this article was based on the terminal perfusion of citrate-treated rats and rats treated with STZ using a reactive ester derivative of biotin (Figure 1a). The terminal perfusion of rodents has previously shown to be a useful technique to identify markers of tumor neo-vasculature, which can be drugged with monoclonal antibodies. The results of this study show that *in vivo* biotinylation facilitates the detection of disease-specific changes in the abundance of accessible proteins in rat kidneys after STZ-induced diabetes. STZ is an analog of N-acetylglucosamine, readily transported into pancreatic β-cells by the glucose transporter GLUT-2 causing β-cell toxicity, leading to insulin deficiency and elevated blood glucose levels. A known limitation of this model is the toxicity of STZ to renal tubular cells. For this study, the standard STZ-induced diabetes model was modified to avoid excessive initial toxic effects and thus to obtain a more manageable diabetes. Further, the earliest time point for the perfusion of rat kidneys was set to 4 weeks in which tubular epithelial cells could regenerate.

Compared with citrate-treated control rats, which showed normal UAERs of about 200 μg per 24 h, the UAER of STZ-treated rats was in the range of 900–1500 μg per 24 h (Supplementary Table S1 online), which is in line with values previously published[32] and which indicates severe kidney damage. The successful *in vivo* protein biotinylation, which was assessed by histochemistry, showed a uniform labeling of glomeruli, blood vessels, and certain tubular structures (Figure 1b). The subsequent mass spectrometry-based

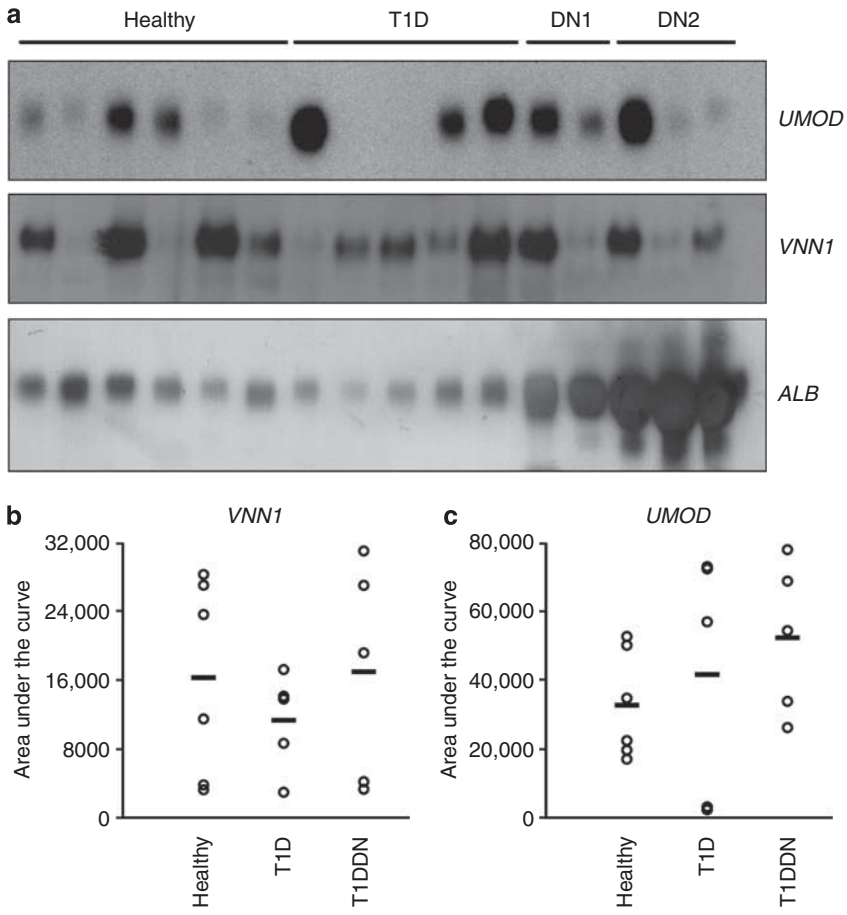

Figure 5 | Quantitative assessment of VNN1 and UMOD in individual urine samples. (**a**) Western blot analyses using urine from healthy individuals (healthy), patients with T1D but normal albumin excretion rates (T1D), and patients with elevated (DN1) and pronounced (DN2) urinary albumin excretion rate (UAER) were performed with antibodies against *UMOD*, *VNN1*, and *ALB*. *VNN1* (**b**) and *UMOD* (**c**) bands were quantified using image J software (US National Institutes of Health, Bethesda, MD). The area under the curve of bands from individual urine samples is displayed as circles, whereas the average in a pathological group is displayed with a horizontal line. For this analysis, all diabetic patients with elevated UAER were included in one group (T1DDN) to have a higher number of measurements per group.

proteomic analysis resulted in the identification and label-free relative quantification of 396 proteins, whereof 24 and 11 proteins were found more than 10-fold upregulated and downregulated in the diseased kidneys compared with the healthy citrate-treated kidneys, respectively (Figure 2, Supplementary Figure S1 online and Supplementary Table S2 online). Several proteins could be mapped to distinct locations in the kidney, such as the glomerular basement membrane, the apical as well as the lateral membrane of the podocyte, the endothelial membrane, and the proximal tubule (Table 1), thereby defining the kidney substructures in which proteins were chemically modified by the reactive ester derivative of biotin. Importantly, most serum components, such as albumin (a known marker for accelerated plasma protein leakage across the glomerular basement membrane in DN), transferrin, and fibrinogen, were not found to be regulated in this proteomic analysis. In contrast, serum components, which were previously identified to be either upregulated in the serum of patients with diabetes (kallikrein,[33] haptoglobin,[34] and coagulation factor XII[33]) or to be associated with DN (kininogen 1 (ref.35)), were found among the most differentially expressed proteins.

The upregulated proteins vanin-1 (*Vnn1*), Enpp6 protein (*Enpp6*), and alpha-1-acid glycoprotein (*Orm1*) were further validated. Although no correlation between the upregulation of *Enpp6* and diabetes or DN was found in literature, the upregulation of *Vnn1* in T1D[36] and of *Orm1* in DN[37] has previously been described. An immunofluorescence analysis of *Enpp6* and *Orm1* on rat kidney section revealed their upregulation in tubular structures and glomeruli in STZ-treated diabetic rats, respectively (Figure 3).

Orm1 could be detected by immunofluorescence staining, which was also confirmed by western blot of rat kidney tissue homogenates (data not shown) but could not be detected in human urine samples.

Enpp6 was found to be expressed on tubular epithelium in kidney sections from STZ-treated rats, but both commercial antibodies tested were reactive against human immunoglobulin G heavy chain, as demonstrated by western blot, detecting purified human immunoglobulin G (data not

shown). Owing to the similar size of the heavy chain (~55 kDa) and *ENPP6* (~52 kDa), and the upregulation of human immunoglobulin G fragments in DN, it was impossible to discriminate between specific and nonspecific signals. Interestingly, *ENPP6* was identified in a study of urinary exosomes,[38] suggesting that this protein is also expressed in healthy kidneys, making it a top candidate for follow-up studies.

Although the immunofluorescence staining of *Vnn1* could not be performed because of the unavailability of antibodies recognizing the rat protein, it showed to be upregulated in pooled urine of T1D patients with macroalbuminuria (Figure 4). In contrast, the analysis of spot urine from individual patients presented a variable *VNN1* concentration, without a significant upregulation in DN patients. These findings could be explained in terms of patient improvement as a result of pharmacological intervention (formerly overt albuminuria indeed reverted to UAER below 300 mg/l). Alternatively, if this protein is indeed of tubular origin, timed urine collections should be considered, as recently proposed,[39] to more reliably assess the rate of protein release. Both issues can only be resolved by studying a larger patient population, with additional time points for urine collection.

Uromodulin (*UMOD;* also known as Tamm–Horsfall urinary glycoprotein) was identified in the proteomic analysis to be downregulated in the diabetic rat samples when compared with the citrate-treated control rats. This is in line with the observation of Chakraborty and co-workers[40] who showed that a decreased immunogold labeling of *UMOD* in human kidney specimens is associated with renal damage and with our immunofluorescence analysis on rat kidneys (Figure 3). The upregulation of *UMOD* in individual and pooled patient urine (Figure 4) seems to be contradictory at first but can be explained by its shedding into the urine, which was proposed to have a role in water/salt balance.[41] The observation that this balance is altered in DN suggests that uromodulin shedding is increased under pathological condition.[42,43]

In this proteomics-based study of a T1D rat model and its complications, we have identified 396 proteins and followed their expression over a time course of 12 weeks. The protein most significantly upregulated in the diabetic rats was vanin-1, a glycosylphosphatidylinositol-anchored epithelial pantetheinase, which has proinflammatory and cytoprotective effects in some tissues.[44,45] Modulation of the vanin-1 activity has been suggested as alternative strategy to maintain islet cell homeostasis.[36] Although vanin-1 is indeed upregulated in a pool of urine from patients with macroalbuminuria, an analysis of individual urine samples showed large interindividual variability, indicating the need for dedicated studies with large numbers of individual urine samples to properly assess the value of this candidate marker for the monitoring of DN progression in patients.

Recently, serum cystatin C has been proposed for the early detection of DN,[46] and is currently evaluated for the detection of mildly to moderately impaired kidney function in diabetic patients. In full analogy to the development of cystatin C, vanin-1 could be validated as marker for the early detection of impaired kidney function in diabetes patients. For this purpose, large-scale studies using clinically validated urine samples of healthy individuals and diabetic patients with different stages of impaired renal function have to be carried out. To perform such studies, specific high-affinity monoclonal antibodies as well as validated antibody-based tests (for example, enzyme-linked immunosorbent assay) are essential and have to be developed, challenges which are clearly beyond the scope of this study.

MATERIALS AND METHODS

Animals

Nine-week-old male Sprague–Dawley rats (Charles River, Wilmington, MA) with known sensitivity to STZ-induced diabetes weighing 268 ± 11 g were used. All animals were housed under standard conditions (light on 08:00–20:00 h; 40–70% relative humidity, 22 ± 1 °C), and had free access to water and chow (Altromin standard diet, Lange, Germany). All procedures were in accordance with the guidelines of the Institutional Animal Care and Use Committee of the Semmelweis University.

DN model

STZ diabetes was induced, as described previously.[47] Briefly, rats obtained a single intraperitoneal injection of 55 mg STZ (N-(methylnitrosocarbamoyl)-α-D-glucosamine; Sigma-Aldrich, St Louis, MO) per kg body weight dissolved in citrate buffer (pH 4.5). Rapid administration of STZ and solution pH is important to achieve diabetes. A total of 17 animals were stratified into four groups ($n = 4$/group) with equal average initial body weight: four groups of animals were injected with STZ, and 5 age-matched control rats were injected with the citrate buffer only.

In vivo biotinylation

In vivo biotinylation experiments were performed similarly, as previously described.[20,26] Briefly, rats were anesthetized with a combination of ketamin (Vétoquinol, Ittingen, Switzerland), xylazin (Streuli, Uznach, Switzerland), and acepromazine (Arovet, Dietikon, Switzerland). The abdomen was opened and two ligations (the first on the abdominal artery and vein below the branching points of the kidney arteries and the second on the hepatic artery) were placed. Following a median sternotomy, a buttoned cannula was inserted into the aorta abdominalis and fixed with medical wire. To allow the biotinylation reagent to flow out, the vena cava was cut open. The perfusion was carried out at 150 mm Hg column using 20 ml prewarmed (40 °C) biotinylation solution (0.5 mg/ml Sulfo-NHS-LC-Biotin (Pierce) and 10% Dextran-40 (GE Healthcare, Chalfont St Giles, UK) in phosphate-buffered saline, followed by 20 ml of prewarmed (40 °C) quenching solution (50 mmol/l Tris-HCl and 10% Dextran-40 in phosphate-buffered saline). After perfusion, kidneys were excised, cut in half, and separately freshly snap frozen in liquid nitrogen-cooled isopentane for preparation of organ homogenates. A total of nine STZ rats and five citrate-treated control rats were terminally perfused. An unperfused citrate-treated rat was used as negative control for the proteomic analysis.

Purification of biotinylated proteins and proteomic analysis

Purification of biotinylated proteins on streptavidin resin, the tryptic on-resin digestion, and the subsequent proteomic analysis of resulting tryptic peptides were performed according to standard

procedures.[22,48] A detailed description can be found in the Supplementary Materials online.

Relative protein quantification by DeepQuanTR software

The DeepQuanTR software has been described in detail elsewhere.[29] Briefly, after mass spectrometry acquisition, data related to the individual peaks (fractions, intensities, and mass-to-charge ratios) were loaded into the DeepQuanTR software, which performed a normalization of individual signal intensities to the internal standard peptides and an annotation (peptide identification and association with a parent protein). Normalized intensities for the individual peptides from all samples of each group (that is, citrate control, 4, 8, and 12 weeks after STZ injection) were used for the computation of DeepQuanTR peptide and protein scores, indicating the relative abundance of individual peptides and proteins in the various groups of samples.

Human urine samples

Human urine samples from healthy individuals were obtained from male volunteers of the lab (midstream morning urine, supplemented with 1 × complete proteinase inhibitor cocktail (Roche Diagnostics, Mannheim, Germany), centrifuged at 3300 × *g* for 10 min at 4 °C, and the supernatant was aliquoted and stored at −80 °C). Human urine from patients with T1D were obtained from the Finnish Diabetic Nephropathy (FinnDiane) Study.[49] Six patients with normal albumin excretion rate (<30 mg/24 h) and six with macroalbuminuria (>300 mg/24 h) provided urine for two pools of urine, respectively. All patients exhibited similar creatinine concentrations. The pools were aliquoted and stored at −20 °C.

For the analysis of interindividual variability of *VNN1* and *UMOD* levels, urine of 10 additional patients was collected, as described above. Five patients were diabetic with UAER <30 mg/l and two patients exhibited elevated albumin levels (>30; <200 mg/l). Three patients suffered from overt albuminuria but because of successful medication, their UAER fell below the threshold of macroalbuminuria at the time of sample collection. All relevant data for the 16 individual urine donors can be found in Supplementary Table S5 online.

A detailed description of the functional measurements, the histochemistry, the preparation of protein extracts, the purification of biotinylated proteins, the proteomic analysis, the immunofluorescence analysis (Supplementary Table S4 online), and the western blot analysis can be found in the Supplementary Materials online.

DISCLOSURE

All the authors declared no competing interests.

ACKNOWLEDGMENTS

This study was financially supported by the Swiss National Science Foundation, the ETH Zürich, the European Union (DiaNa project LSHB-CT-2006-037681), the SwissBridge Foundation, and the Stammbach. We thank the Functional Genomics Center Zurich for access to the high-performance liquid chromatography and for technical support. Support was provided to PH from the Hungarian Research Fund (OTKA NF69278). The FinnDiane Study was funded by the Folkhälsan Research Foundation, Wilhelm and Else Stockmann Foundation, Sigrid Juselius Foundation, Medicinska Understödsföreningen Liv och Hälsa, Signe and Ane Gyllenberg Foundation, and EVO governmental grants.

AUTHOR CONTRIBUTIONS

TF performed experiments, analyzed data, and wrote the manuscript. BB performed perfusion experiments. CsR set up the rat diabetes model. MG performed the rat *in vitro* functional analysis. CF provided validated urine samples of diabetic patients. PH planned and supervised the setup of the rat diabetes model and wrote the manuscript. HH designed the project and reviewed the manuscript. DN designed the project, analyzed data, wrote, and reviewed the manuscript. ChR designed the project, performed experiments, analyzed data, and wrote the article.

SUPPLEMENTARY MATERIAL

Table S1. Specification of functional data obtained at 12 weeks after streptozotocin (STZ) or citrate treatment in the Sprague–Dawley rats.
Table S2. Total list of proteins identified with at least two proteotypic peptides in the comparative proteomic analysis.
Table S3. Comparison of protein regulation in diabetic nephropathy between a transcriptomic study (data based on human mRNA expression profiles of diabetic glomeruli and glomeruli from healthy individuals) and this proteomic study (data based on protein expression in STZ rats and healthy citrate-treated rats).
Table S4. Summary of the antibodies used for immunofluorescence analysis and/or western blotting.
Table S5. Clinical data of healthy individuals and patients with type 1 diabetes.
Figure S1. Cluster analysis.
Figure S2. Correlation between microarray data (Rudnicki *et al.*[30]) and the proteomics data presented in this work.
Supplementary material is linked to the online version of the paper at http://www.nature.com/ki

REFERENCES

1. Daneman D. Type 1 diabetes. *Lancet* 2006; **367**: 847–858.
2. Devendra D, Liu E, Eisenbarth GS. Type 1 diabetes: recent developments. *BMJ* 2004; **328**: 750–754.
3. Reeves WB, Andreoli TE. Transforming growth factor beta contributes to progressive diabetic nephropathy. *Proc Natl Acad Sci USA* 2000; **97**: 7667–7669.
4. Fioretto P, Mauer M. Histopathology of diabetic nephropathy. *Seminars in Nephrology* 2007; **27**: 195–207.
5. Raptis AE, Viberti G. Pathogenesis of diabetic nephropathy. *Exp Clin Endocrinol Diabetes* 2001; **109**(Suppl 2): S424–S437.
6. Hostetter TH, Rennke HG, Brenner BM. The case for intrarenal hypertension in the initiation and progression of diabetic and other glomerulopathies. *Am J Med* 1982; **72**: 375–380.
7. Chang SS. Albuminuria and diabetic nephropathy. *Pediatr Endocrinol Rev* 2008; **5**(Suppl 4): 974–979.
8. Crawford PW, Lerma EV. Treatment options for end stage renal disease. *Prim Care* 2008; **35**: 407–432, v.
9. Bianchi S, Bigazzi R, Campese VM. Microalbuminuria in essential hypertension: significance, pathophysiology, and therapeutic implications. *Am J Kidney Dis* 1999; **34**: 973–995.
10. Steinke JM, Sinaiko AR, Kramer MS *et al.* The early natural history of nephropathy in Type 1 Diabetes: III. Predictors of 5-year urinary albumin excretion rate patterns in initially normoalbuminuric patients. *Diabetes* 2005; **54**: 2164–2171.
11. Caramori ML, Kim Y, Huang C *et al.* Cellular basis of diabetic nephropathy: 1. Study design and renal structural-functional relationships in patients with long-standing type 1 diabetes. *Diabetes* 2002; **51**: 1294.
12. Cooper ME, Allen TJ, Macmillan P *et al.* Genetic hypertension accelerates nephropathy in the streptozotocin diabetic rat. *Am J Hypertens* 1988; **1**: 5–10.
13. Epstein PN, Overbeek PA, Means AR. Calmodulin-induced early-onset diabetes in transgenic mice. *Cell* 1989; **58**: 1067–1073.
14. Sharma K, Lee S, Han S *et al.* Two-dimensional fluorescence difference gel electrophoresis analysis of the urine proteome in human diabetic nephropathy. *Proteomics* 2005; **5**: 2648–2655.
15. Cho WC, Yip TT, Chung WS *et al.* Differential expression of proteins in kidney, eye, aorta, and serum of diabetic and non-diabetic rats. *J Cell Biochem* 2006; **99**: 256–268.
16. Thongboonkerd V, Barati MT, McLeish KR *et al.* Alterations in the renal elastin-elastase system in type 1 diabetic nephropathy identified by proteomic analysis. *J Am Soc Nephrol* 2004; **15**: 650–662.
17. Sitek B, Potthoff S, Schulenborg T *et al.* Novel approaches to analyse glomerular proteins from smallest scale murine and human samples using DIGE saturation labelling. *Proteomics* 2006; **6**: 4337–4345.

18. Schordan S, Schordan E, Endlich N *et al.* Alterations of the podocyte proteome in response to high glucose concentrations. *Proteomics* 2009; **9**: 4519–4528.
19. Borgia B, Roesli C, Fugmann T *et al.* A proteomic approach for the identification of vascular markers of liver metastasis. *Cancer Res* 2009.
20. Rybak JN, Ettorre A, Kaissling B *et al. In vivo* protein biotinylation for identification of organ-specific antigens accessible from the vasculature. *Nat Methods* 2005; **2**: 291–298.
21. Rybak JN, Roesli C, Kaspar M *et al.* The extra-domain A of fibronectin is a vascular marker of solid tumors and metastases. *Cancer Res* 2007; **67**: 10948–10957.
22. Schliemann C, Roesli C, Kamada H *et al. In vivo* biotinylation of the vasculature in B cell lymphoma identifies BST-2 as a target for antibody-based therapy. *Blood* 2009; **115**: 736–744.
23. Castronovo V, Waltregny D, Kischel P *et al.* A chemical proteomics approach for the identification of accessible antigens expressed in human kidney cancer. *Mol Cell Proteomics* 2006; **5**: 2083–2091.
24. Conrotto P, Roesli C, Rybak J *et al.* Identification of new accessible tumor antigens in human colon cancer by *ex vivo* protein biotinylation and comparative mass spectrometry analysis. *Int J Cancer* 2008; **123**: 2856–2864.
25. Villa A, Trachsel E, Kaspar M *et al.* A high-affinity human monoclonal antibody specific to the alternatively spliced EDA domain of fibronectin efficiently targets tumor neo-vasculature *in vivo*. *Int J Cancer* 2008; **122**: 2405–2413.
26. Roesli C, Neri D, Rybak JN. *In vivo* protein biotinylation and sample preparation for the proteomic identification of organ- and disease-specific antigens accessible from the vasculature. *Nat Protoc* 2006; **1**: 192–199.
27. Roesli C, Elia G, Neri D. Two-dimensional mass spectrometric mapping. *Curr Opin Chem Biol* 2006; **10**: 35–41.
28. Scheurer SB, Rybak JN, Roesli C *et al.* Identification and relative quantification of membrane proteins by surface biotinylation and two-dimensional peptide mapping. *Proteomics* 2005; **5**: 2718–2728.
29. Fugmann T, Neri D, Roesli C. DeepQuanTR: MALDI-MS-based label-free quantification of proteins in complex biological samples. *Proteomics* 2010; **10**: 2631–2643.
30. Rudnicki M, Eder S, Perco P *et al.* Gene expression profiles of human proximal tubular epithelial cells in proteinuric nephropathies. *Kidney Int* 2007; **71**: 325–335.
31. Schmid H, Boucherot A, Yasuda Y *et al.* Modular activation of nuclear factor-kappaB transcriptional programs in human diabetic nephropathy. *Diabetes* 2006; **55**: 2993–3003.
32. Cadaval RA, Kohlman O, Michelacci YM. Urinary excretion of glycosaminoglycans and albumin in experimental diabetes mellitus. *Glycobiology* 2000; **10**: 185–192.
33. Carr ME. Diabetes mellitus: a hypercoagulable state. *J Diabetes Complications* 2001; **15**: 44–54.
34. Dincer A, Onal S, Timur S *et al.* Differentially displayed proteins as a tool for the development of type 2 diabetes. *Ann Clin Biochem* 2009; **46**: 306–310.
35. Vionnet N, Tregouet D, Kazeem G *et al.* Analysis of 14 candidate genes for diabetic nephropathy on chromosome 3q in European populations: strongest evidence for association with a variant in the promoter region of the adiponectin gene. *Diabetes* 2006; **55**: 3166–3174.
36. Roisin-Bouffay C, Castellano R, Valero R *et al.* Mouse vanin-1 is cytoprotective for islet beta cells and regulates the development of type 1 diabetes. *Diabetologia* 2008; **51**: 1192–1201.
37. Jiang H, Guan G, Zhang R *et al.* Increased urinary excretion of orosomucoid is a risk predictor of diabetic nephropathy. *Nephrology (Carlton)* 2009; **14**: 332–337.
38. Pisitkun T, Shen RF, Knepper MA. Identification and proteomic profiling of exosomes in human urine. *Proc Natl Acad Sci USA* 2004; **101**: 13368–13373.
39. Waikar SS, Sabbisetti VS, Bonventre JV. Normalization of urinary biomarkers to creatinine during changes in glomerular filtration rate. *Kidney Int* 2010; **78**: 486–494.
40. Chakraborty J, Below AA, Solaiman D. Tamm-Horsfall protein in patients with kidney damage and diabetes. *Urol Res* 2004; **32**: 79–83.
41. Wiggins RC. Uromucoid (Tamm-Horsfall glycoprotein) forms different polymeric arrangements on a filter surface under different physicochemical conditions. *Clin Chim Acta* 1987; **162**: 329–340.
42. Agardh CD, Stenram U, Torffvit O *et al.* Effects of inhibition of glycation and oxidative stress on the development of diabetic nephropathy in rats. *J Diabetes Complications* 2002; **16**: 395–400.
43. Hong CY, Chia KS. Markers of diabetic nephropathy. *J Diabetes Complications* 1998; **12**: 43–60.
44. Berruyer C, Pouyet L, Millet V *et al.* Vanin-1 licenses inflammatory mediator production by gut epithelial cells and controls colitis by antagonizing peroxisome proliferator-activated receptor gamma activity. *J Exp Med* 2006; **203**: 2817–2827.
45. Karpuj MV, Becher MW, Springer JE *et al.* Prolonged survival and decreased abnormal movements in transgenic model of Huntington disease, with administration of the transglutaminase inhibitor cystamine. *Nat Med* 2002; **8**: 143–149.
46. Lee BW, Ihm SH, Choi MG *et al.* The comparison of cystatin C and creatinine as an accurate serum marker in the prediction of type 2 diabetic nephropathy. *Diabetes Res Clin Pract* 2007; **78**: 428–434.
47. Rakieten N, Rakieten ML, Nadkarni MV. Studies on the diabetogenic action of streptozotocin (NSC-37917). *Cancer Chemother Rep* 1963; **29**: 91–98.
48. Borgia B, Roesli C, Fugmann T *et al.* A proteomic approach for the identification of vascular markers of liver metastasis. *Cancer Res* 2010; **70**: 309–318.
49. Thorn LM, Forsblom C, Fagerudd J *et al.* Metabolic syndrome in type 1 diabetes: association with diabetic nephropathy and glycemic control (the FinnDiane study). *Diabetes Care* 2005; **28**: 2019–2024.
50. Woodfin A, Voisin MB, Nourshargh S. PECAM-1: a multi-functional molecule in inflammation and vascular biology. *Arterioscler Thromb Vasc Biol* 2007; **27**: 2514–2523.
51. Pellet-Many C, Frankel P, Jia H *et al.* Neuropilins: structure, function and role in disease. *Biochem J* 2008; **411**: 211–226.
52. Wong KS, Proulx K, Rost MS *et al.* Identification of vasculature-specific genes by microarray analysis of Etsrp/Etv2 overexpressing zebrafish embryos. *Dev Dyn* 2009; **238**: 1836–1850.
53. Aaltonen P, Holthofer H. The nephrin-based slit diaphragm: new insight into the signalling platform identifies targets for therapy. *Nephrol Dial Transplant* 2007; **22**: 3408–3410.
54. Karamatic Crew V, Burton N, Kagan A *et al.* CD151, the first member of the tetraspanin (TM4) superfamily detected on erythrocytes, is essential for the correct assembly of human basement membranes in kidney and skin. *Blood* 2004; **104**: 2217–2223.
55. Li JJ, Kwak SJ, Jung DS *et al.* Podocyte biology in diabetic nephropathy. *Kidney Int Suppl* 2007; **106**: S36–S42.
56. Raciti D, Reggiani L, Geffers L *et al.* Organization of the pronephric kidney revealed by large-scale gene expression mapping. *Genome Biol* 2008; **9**: R84.